

Structure/Function Relationships in Dyes for Solar Energy Conversion: A Two-Atom Change in Dye Structure and the Mechanism for Its Effect on Cell Voltage

Brian C. O'Regan,* Kate Walley, Mindaugas Juozapavicius, Assaf Anderson, Farah Matar, Tarek Ghaddar,* Shaik M. Zakeeruddin, Cédric Klein, and James R. Durrant

Department of Chemistry, Imperial College London, London SW7 2AZ, United Kingdom, Department of Chemistry, American University of Beirut, Beirut, 11-0236 Lebanon, and Laboratory for Photonics & Interfaces, Swiss Federal Institute of Technology, CH 1015, Lausanne, Switzerland

Received August 29, 2008; E-mail: b.oregan@imperial.ac.uk; tg02@aub.edu.lb

Abstract: Recombination between injected electrons and iodine limits the photovoltage in dye-sensitized solar cells (DSSCs). We have recently suggested that many new dye molecules, intended to improve DSSCs, can accelerate this reaction, negating the expected improvement (*J. Am. Chem. Soc.* **2008**, *130*, 2907). Here we study two dyes with only a two-atom change in the structure, yet which give different V_{oc} s. Using a range of measurements we show conclusively that the change in V_{oc} is due solely to the increase in the recombination rate. From the structure of the dyes, and literature values for iodine binding of similar compounds, we find that it is very likely that the change in V_{oc} is due solely to the difference in iodine binding at the site of the two-atom change. Using the large amount of literature on iodine complexation, we suggest structures for dyes that might show improved V_{oc} .

Introduction

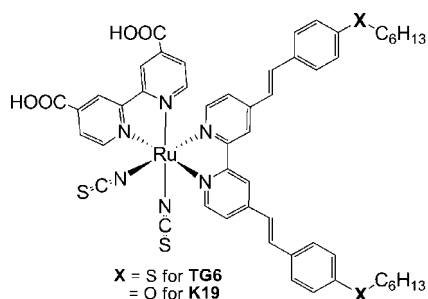
Dye-sensitized solar cells (DSSCs) are suggested as a lower cost alternative to silicon-based photovoltaics (PVs).^{1,2} Dye-sensitized cells can be manufactured with lower purity, and therefore lower cost, materials compared to silicon cells. Record efficiencies for dye-sensitized cells (~11%) are lower than those for silicon cells (~24%).³ Despite this difference, several companies are reported to be developing DSSC modules, and one company (G42i) is producing flexible DSSC modules in a roll-to-roll process. To become more competitive with Si-based PVs, and also to contribute significantly to world energy needs, the efficiency of DSSCs needs to be improved. One of the possible avenues for improving DSSCs is to increase the fraction of the solar spectrum that is absorbed by the dye. At present, the best dyes absorb light only weakly beyond 700 nm. For example, the absorption spectrum of a current benchmark dye, N719 (*cis*-dithiocyanato-bis(2,2'-bipyridyl-4,4'-dicarboxylate)-ruthenium(II)), is shown in Figure 1.⁴ Extending this absorption to the red by 100 nm, without losing efficiency in other ways, would result in a significant improvement in photocurrent. However, over the past 15 years, possibly 1000 different dyes have been tested, and the result "without losing efficiency in other ways" has not yet been realized. Although this track record might seem dispiriting, it must be kept in mind that the number

of possible dyes is nearly infinite. We believe that the lack of significant progress reflects not only the inherent difficulty of the project but also that the effects of dye structure on all the processes taking place in the cell are much more complex than originally appreciated.

We have recently found evidence that many, or even most, dyes can have a role in promoting electron recombination with iodine in DSSCs.⁵ Acceleration of this recombination lowers the V_{oc} , and thus the efficiency. A role for the dye is at first glance surprising as the dye is not involved in the overall reaction of recombination. Moreover, such a role is a reversal of previous thought, where the dye has been considered to be a blocking layer with respect to recombination. From our previous results, we were led to propose that phthalocyanines, at least, may accelerate recombination by providing a binding site for iodine near the TiO₂ surface.⁵ A similar binding has been previously suggested for porphyrins⁶ and some ruthenium complex dyes.⁷ In light of these developments we have undertaken a larger study of dyes for DSSCs in order to better understand the cause of the recombination rate increase seen. This is part of our ongoing work on structure/function relations in DSSCs, including also the effect of dye structure on electron injection and dye regeneration.^{5,8–11}

- (1) O'Regan, B.; Grätzel, M. *Nature* **1991**, *353*, 737.
- (2) Kroon, J. M.; et al. *Prog. Photovoltaics* **2007**, *15*, 1.
- (3) Chiba, Y.; Islam, A.; Watanabe, Y.; Komiya, R.; Koide, N.; Han, L. Y. *Jpn. J. Appl. Phys., Part 2* **2006**, *45*, L638.
- (4) Nazeeruddin, M. K.; Kay, A.; Rodicio, I.; Humphry-Baker, R.; Muller, E.; Liska, P.; Vlachopoulos, N.; Grätzel, M. *J. Am. Chem. Soc.* **1993**, *115*, 6382.

- (5) O'Regan, B. C.; López-Duarte, I.; Martínez-Díaz, M. V.; Forneli, A.; Albero, J.; Morandiera, A.; Palomares, E.; Torres, T.; Durrant, J. R. *J. Am. Chem. Soc.* **2008**, *130*, 2907.
- (6) Splan, K. E.; Massari, A. M. T.; Hupp, J. T. *J. Phys. Chem. B* **2004**, *108*, 4111.
- (7) Clark, C. C.; Marton, A.; Srinivasan, R.; Sarjeant, A. A. N.; Meyer, G. J. *Inorg. Chem.* **2006**, *45*, 4728.
- (8) Koops, S. E.; Durrant, J. R. *Inorg. Chim. Acta* **2008**, *361*, 663.

Scheme 1. Structure of TG6 (X = S) and K19 (X = O) Dyes

In this paper we report the effects on recombination of two very similar dyes, TG6 and K19, where two identical oxygen atoms on K19 have been changed to two sulfur atoms on TG6 (Scheme 1).^{12,13} The dyes were chosen because the oxygen/sulfur difference should change the iodine binding, but leaves most other properties relatively unaffected. Using this model system, we can quantify the effect of a two-atom change on recombination. The results illustrate the subtlety of the structure/function relationship in DSSCs. In this case, a change of an oxygen to sulfur in two equivalent positions, out of a total molecular size of 113 atoms, gives a 2-fold increase in the recombination rate and a 20–30 mV loss in V_{oc} . Because the two-atom change can be correlated with a change in literature values for iodine binding, the results strongly support our original hypothesis that binding of iodine to the dye is a key element of the recombination process in DSSCs.

In dye-sensitized cells, light absorption occurs in a monolayer of dye at the interface between a transparent oxide electron conductor (usually TiO_2) and a transparent electrolyte. Sufficient light absorption is achieved by using a thick film ($\sim 10 \mu m$) of nanosized oxide particles (~ 20 nm) wherein all the internal surface of the film is coated with the dye. A liquid electrolyte is introduced into the pores containing a redox couple, virtually always iodine/iodide in an organic solvent. The TiO_2 layer is commonly supported on a transparent conductive contact, usually fluorine-doped tin oxide (FTO) on glass, so that light can be introduced from the “ TiO_2 ” side of the device. The device is completed by placing another FTO glass “counter electrode” facing the TiO_2 -coated electrode with a $\sim 20 \mu m$ gap between the two electrodes. The edges are sealed to prevent evaporation or contamination of the electrolyte. This arrangement was used for the cells studied in this paper. We note that there are other physical arrangements for DSSCs. In some prototype modules, the TiO_2 layer is supported on opaque metal foil, and light is introduced from the electrolyte side of the cell through a transparent counter electrode. All designs, however, follow the same basic rules of operation.

The functioning of DSSCs has been described, and only relevant details will be repeated herein.^{14,15} The forward (desired) processes are as follows. After light absorption by the dye, the excited dye injects an electron into the TiO_2 . The thus

photo-oxidized dye is then regenerated (returned to the original state) by oxidizing an iodide ion in solution. The net outcome of the absorption of two photons is the creation of two additional electrons in the TiO_2 and one additional iodine molecule in solution. During operation, the electrons diffuse to the FTO contact, from where they flow to the external circuit, through the load, and to the counter electrode. The excess iodine diffuses to the counter electrode, where it is reduced to iodide. Diffusion of iodide back into the pores of the TiO_2 layer completes the circuit. Quantum efficiency and energy losses can of course occur at any step of this process. For a general description of losses, see ref 15.

One important loss route is the recombination of electrons in the TiO_2 with iodine. The rate constant for this recombination is one of the factors which control the open-circuit voltage of the cell. When iodine and iodide are mixed, there is a strong complexation to make I_3^- (tri-iodide).¹⁶ When iodide is in excess, as in these cells, almost all the iodine is present as tri-iodide. It is not yet certain whether the first electron-transfer step in the recombination involves the reduction of iodine or tri-iodide, or perhaps both in some ratio. We will use “iodine” from this point on, with the understanding that we mean iodine or possibly tri-iodide. The output voltage of the DSSC under operation is the difference between the Fermi level in the TiO_2 and the redox potential of the electrolyte. When light is applied to the cell, the dyes begin to inject electrons into the TiO_2 , and the concentration of electrons in the TiO_2 increases. This causes the Fermi level in the TiO_2 to move away from the potential of the electrolyte, establishing the potential difference. As the concentration of electrons increases, the recombination rate of the electrons with the iodine increases. At open circuit, by definition, the concentration of electrons has increased to the point where the flux of recombining electrons equals the flux of injected electrons ($J_{rec} = J_{inj}$). This concentration of electrons in turn fixes the Fermi level in the TiO_2 and thus the V_{oc} .

In DSSC cells, the recombination flux follows the form $J_{rec} = k_0 n^\alpha [I_{os}]^\beta$, where n is the total concentration of electrons in the system (trapped and conduction band) and $[I_{os}]$ is the near surface concentration of oxidized iodide in the electrolyte (I_2 and/or I_3^-). The value β is still under some debate; values of 1 or 2 are suggested from the literature.^{17–19} The value of α depends on the trap distribution and thus varies for different preparations; for the cells used herein $\alpha \approx 3.6$. It is clear that if something causes $[I_{os}]$ or k_0 to increase, the condition $J_{rec} = J_{inj}$ will occur at a lower n . A lower n will give a lower Fermi level in the TiO_2 , and thus a lower V_{oc} . We cannot measure $[I_{os}]$ directly; however, our measurements can quantify changes in the product $k_0 [I_{os}]$, which we will refer to as k_0' . To quantify changes in k_0' we measure the electron lifetime and charge density. By definition, the electron lifetime is the inverse of the pseudo-first-order rate constant, $\tau = 1/k_{pfo}$, and also $J_{rec} = k_{pfo} n$. From this we see that $k_{pfo} = k_0' n^{\alpha-1}$. Thus, when compared at the same electron density, the ratio of the lifetimes of two

- (9) Clifford, J. N.; Palomares, E.; Nazeeruddin, M. K.; Grätzel, M.; Durrant, J. R. *J. Phys. Chem. C* **2007**, *111*, 6561.
 (10) Morandeira, A.; Lopez-Duarte, I.; Martinez-Diaz, M. V.; O'Regan, B.; Shuttle, C.; Haji-Zainulabidin, N. A.; Torres, T.; Palomares, E.; Durrant, J. R. *J. Am. Chem. Soc.* **2007**, *129*, 9250.
 (11) Green, A. N. M.; Palomares, E.; Haque, S. A.; Kroon, J. M.; Durrant, J. R. *J. Phys. Chem. B* **2005**, *109*, 12525.
 (12) Matar, F.; Ghaddar, T. H.; Walley, K.; DosSantos, T.; Durrant, J. R.; O'Regan, B. C. *J. Mater. Chem.* **2008**, *18*, 4246.
 (13) Wang, P.; Klein, C.; Humphry-Baker, R.; Zakeeruddin, S. M.; Grätzel, M. *J. Am. Chem. Soc.* **2005**, *127*, 808.

- (14) Peter, L. M. *J. Phys. Chem. C* **2007**, *111*, 6601.
 (15) O'Regan, B.; Durrant, J. R.; Sommeling, P.; Bakker, N. J. *J. Phys. Chem. C* **2007**, *111*, 14001.
 (16) Baucke, F. G. K.; Bertram, R.; Cruse, K. *Electroanal. Chem. Interfacial Electrochem.* **1971**, *32*, 247.
 (17) Huang, S. Y.; Schlichthorl, G.; Nozik, A. J.; Grätzel, M.; Frank, A. J. *J. Phys. Chem. B* **1997**, *101*, 2576.
 (18) Liu, Y.; Hagfeldt, A.; Xiao, X. R.; Lindquist, S. E. *Sol. Energy Mater. Sol. Cells* **1998**, *55*, 267.
 (19) Green, A. N. M.; Chandler, R. E.; Haque, S. A.; Nelson, J.; Durrant, J. R. *J. Phys. Chem. B* **2005**, *109*, 142.

cells is the same as the ratio of the k_0' 's. We will use graphs of τ vs n to present differences in recombination rates. The separation of changes in k_0' into changes in $[I_{0s}]$ and k_0 is treated in the Discussion.

Another factor controlling the output voltage is the potential of the energy levels inside the TiO_2 (conduction band and traps) relative to the redox potential of the electrolyte. Changes in the surface potential of the TiO_2 , and/or in the trap density in the TiO_2 , will also change the relationship between a particular electron concentration and the resultant Fermi level and V_{oc} . By plotting n vs V_{oc} , we can estimate the shifts in the conduction band potential and separate the effects of a given dye on the surface potential and recombination rate.

Using these techniques we can quantify the difference between the two dyes TG6 and K19 mentioned above (Scheme 1). These two dyes were originally designed to have higher absorption coefficients and to be slightly red shifted relative to N719. The higher absorption coefficient in the red tail of the absorption spectrum can allow greater light absorption and hopefully an increased photocurrent. The higher absorption coefficient in general can allow a decrease in the number of dyes required to fully absorb the sunlight. This makes it possible to use a thinner TiO_2 layer, which in turn makes it easier to fabricate more reproducible and more stable cells. All these can decrease the eventual cost of the cell. However, in both these dyes, there is a significant loss of voltage relative to N719 in an otherwise identical cell, limiting their usefulness. By studying the small but clear difference between TG6 and K19, we can in turn comment on the larger difference between them and N719 and offer potential routes to overcome their disadvantages.

Experimental Section

Cells were fabricated as in previous studies.^{15,20} Transparent conductive SnO_2 glass, LOF Tec 15, was purchased from Pilkington. TiO_2 particles were synthesized from titanium isopropoxide following the nitric acid/acetic acid route, followed by autoclaving.^{21,22} A stable "paste" of the particles was formed by suspension in a mixture of terpinol and ethylcellulose.²³ Layers of the TiO_2 particles ($\sim 4 \mu\text{m}$) were deposited on the FTO glass by tape casting (also known as "doctor blading"). The TiO_2 layers were heated to 450°C in air for 30 min. An additional $\sim 1 \text{ nm}$ TiO_2 layer over each particle was applied by soaking the TiO_2 films in 50 mM TiCl_4 solution for 30 min at 70°C , followed by a water rinse.^{15,24} For some samples the TiCl_4 treatment was done using a 40 mM TiCl_4 -THF complex solution in water, also for 30 min at 70°C . The TiO_2 film was reheated to 450°C after the TiCl_4 treatment. The film was allowed to cool to $\sim 100^\circ\text{C}$ and then immersed in the dye solution for 12–14 h. The dye N719 was purchased from DyeSol. The dyes TG6 and K19 were synthesized as described previously.^{12,13} A platinized FTO sheet was used as a counter electrode. The cell active area was $1 \times 1 \text{ cm}$. The electrolyte was composed of methoxypropionitrile (MPN) with 0.6 M propylmethylimidazolium iodide, 0.1 M LiI, 0.1 M *tert*-butylpyridine, and 0.25 M iodine. All materials were used as supplied except MPN, which was distilled once under vacuum.

Current vs voltage data were collected using a simulated AM1.5 spectrum with an integrated intensity of 83 mW/cm^2 . The simulator has been cross checked with two outside laboratories (ECN and EPFL). Recombination, transport, and charge density data were measured using a home-built transient electrical and optical system, related to that in previous publications.^{15,20} Bias illumination was provided by 10 white 1 W LEDs with focusing optics (Lumileds). The white LED emission spectrum includes two peaks and covers the range from 420 to 700 nm. The LEDs were mounted on a custom heat sink that focuses the LEDs on one spot at a distance of 20 cm. LEDs were switched with MOSFET switches with switching times of $\sim 20 \text{ ns}$. The turn-off time of the LEDs is 100–200 ns. The bias light intensity was controlled by varying the applied current using a GPIB programmable power supply. Flash illumination was supplied by five similar red LEDs (640 nm, fwhm 25 nm). The solar cell under test was mounted on an $8 \times 8 \times 2 \text{ cm}$ aluminum block for temperature stabilization. The cell was switched between open and short circuit with a MOSFET switch as above. Cell currents were measured over a 2Ω resistor. The cell and lamp switches were controlled by the output of a data acquisition and control card (National Instruments) via a home-programmed interface using Igor software (Wavemetrics).

Recombination time constants were measured by applying a constant white bias light to the cell at open circuit and allowing the voltage (V_{oc}) to stabilize for an equilibration period. After equilibration, a $50 \mu\text{s}$ light pulse was applied to the cell from the red LEDs, while the white bias light remained constant. The flash causes an additional injection of electrons into the TiO_2 . The small increase in electron concentration in the film causes a small increase in output voltage. This voltage decays exponentially back to the equilibrium V_{oc} . Voltage transient peaks were kept below 5 mV by decreasing the pulse length. We fit the decay to extract a pseudo-first-order lifetime of the electron, τ_{tr} . This "transient" time constant differs by a proportionality constant from the true "steady-state" electron lifetime at the given V_{oc} , τ_{ss} , as will be discussed below. A series of 15 light levels was used, between $\sim 90 \text{ mW/cm}^2$ and dark, to give a range of V_{oc} values between the "1 sun" V_{oc} and as close to zero as possible. The light levels were scanned down from $\sim 90 \text{ mW/cm}^2$ and back up to check for hysteresis. We note that some hysteresis is usually present for points at lower light levels. It is known that cells with LiI undergo changes when held at V_{oc} , which can take a long time to remove in the dark.²⁵ In cases of hysteresis we use the points from the decreasing bias light scan. In order to mitigate the hysteresis, the equilibration time was also varied. At a bias light level of 90 mW/cm^2 the equilibration time was 4 s. This was increased to 40 s by 1 mW/cm^2 , and at zero bias light the equilibration time was up to 20 min.

The excess electron density in the film at V_{oc} , relative to short circuit in the dark, was measured using a variant of the charge extraction technique.²⁶ Again, a white bias light was applied to the cell, at open circuit, for a given equilibration time. Then, simultaneously, the cell was switched to short circuit, and the bias light was turned off. The switch to short circuit allows the charge stored in the cell at V_{oc} to flow through the external circuit. Simultaneously removing the bias light ensures no further charge is created. Integration of the discharge current gives a measurement of the total charge present in the cell at the given V_{oc} . A blank experiment where the cell is switched without bias light is used to correct for switching noise and bias currents in the equipment. Again we used 15 light levels between $\sim 90 \text{ mW/cm}^2$ and dark, and scanned the bias light levels downward and upward to check for hysteresis. Depending on the cell components, hysteresis can be present at lower voltages. In addition, we have found that the charge collected during charge extraction increases with the length of the equilibration time under light. Based on our measurements, the

- (20) O'Regan, B.; Bakker, N. J.; Kroeze, J. E.; Smit, H. J. P.; Sommeling, P.; Durrant, J. J. *Phys. Chem. B* **2006**, *110*, 17155.
- (21) Anderson, M. A.; Gieselmann, M. J.; Xu, Q. *J. Membr. Sci.* **1988**, *39*, 243.
- (22) Barbé, C. J.; Arendse, F.; Comte, P.; Jirousek, M.; Lenzmann, F.; Shklover, V.; Grätzel, M. *J. Am. Ceram. Soc.* **1997**, *80*, 3157.
- (23) Spath, M.; Sommeling, P. M.; van Roosmalen, J. A. M.; Smit, H. J. P.; van der Burg, N. P. G.; Mahieu, D. R.; Bakker, N. J.; Kroon, J. M. *Prog. Photovoltaics* **2003**, *11*, 207.
- (24) Sommeling, P. M.; O'Regan, B. C.; Haswell, R. R.; Smit, H. J. P.; Bakker, N. J.; Smits, J. J. T.; Kroon, J. M.; van Roosmalen, J. A. M. *J. Phys. Chem. B* **2006**, *110*, 19191.

- (25) Kopidakis, N.; Benkstein, K. D.; van de Lagemaat, J.; Frank, A. J. *J. Phys. Chem. B* **2003**, *107*, 11307.
- (26) Duffy, N. W.; Peter, L. M.; Rajapakse, R. M. G.; Wijayantha, K. G. U. *Electrochem. Commun.* **2000**, *2*, 658.

difference between a few seconds and 40 s was significant ($>30\%$), but the increase in charge between 40 s and 2 min equilibration was smaller ($\sim 5\%$). In order to complete the experiment in a reasonable time, we have chosen 40 s as the equilibration time for charge extraction.

It has been common in dye-sensitized research publications to present the time constants from transient voltage decays, or from impedance data, τ_{tr} , as the correct "steady-state" electron lifetime for the given conditions. As the underlying rate equation is higher than first order in electrons, this is not correct. When the recombination process is of order α , the actual electron lifetime at steady state is longer than the "transient determined" lifetime by the factor α ; thus, $\tau_{ss} = \tau_{tr}\alpha$. A discussion of this relation can be found in most introductory physical chemistry texts. A more general derivation is in ref 27. As we have measured both charge and lifetime data, we can determine α directly. For the cells used herein, we find $\alpha = 3.6$. In this paper we break with past practice in order to report the corrected lifetimes, τ_{ss} . Because of this, the lifetimes in Figure 5 will appear to be longer than those presented in our earlier papers and those of others. We feel it is important to report the corrected lifetimes in order to more accurately compare recombination across different cells, using different dyes, different TiO_2 s, and different electrolytes. Each of these can cause some change in the apparent order of the reaction and thus in the correction factor. Direct use of transient (or impedance) time constants may cause errors in interpretation when comparing recombination rates that differ by factors less than ~ 3 . We expect that close quantitative comparisons will become more frequent as the field begins to optimize cell performance more carefully.

We note that the overall order of the reaction for electrons, $\alpha \approx 3.6$ for these cells, is unlikely to be due to the reaction mechanism at the point of electron transfer. The apparent order in the reaction is more likely related to the fact that most electrons occupy traps in the TiO_2 . Detrapping to and recombination from the conduction band can create non-integer reaction orders. However, at present there is no adequate theory that gives the quantitatively correct order. Reaction from traps with arbitrarily varying recombination rates as a function of potential can also create any arbitrary reaction order, but there is as yet no experiment to verify the assumptions in this kind of model.²⁸ Lastly, as all measurements have been done with the same concentration of iodine and iodide, we can ignore the effect of changes in bulk iodine concentration on the V_{oc} . If, as we propose below, the binding of iodine to the dye is a key determinant of the overall recombination rate, the order of the reaction in bound and unbound iodine will be important values to determine in the future.

Results

The absorption spectra of TG6, K19, and N719 in solution are shown in Figure 1. The spectra have been normalized at the peak of the visible light transition for each dye to highlight the similarity of this transition across the dyes. The extinction coefficients at the visible peak are as follows: TG6, 23 400; K19, 18 200; and N719, 14 200 $\text{M}^{-1} \text{cm}^{-1}$.^{4,12,13} A small red shift is visible for K19 and TG6 relative to N719. However, for solvatochromic dyes such as these, small spectral shifts in solution are not necessarily reproduced in the spectral response of the cell. Figure 2 shows the incident photon to current efficiency (IPCE) spectrum of K19 and TG6 incorporated in DSSCs. Within the accuracy of our measurements the spectral responses of the two dyes are identical. The spectral response of N719 also peaks at 535 nm in identical electrolytes. After correction for reflection and absorption of the front FTO glass

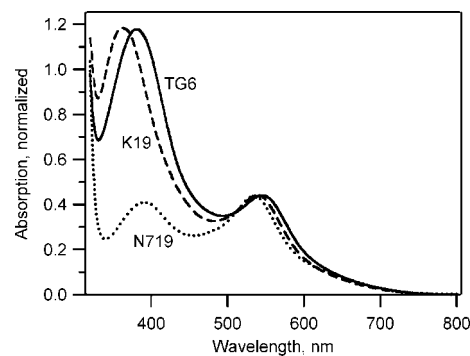


Figure 1. Absorption spectra of TG6, K19, and N719. Normalized to the visible transition. Solvents: N719 and K19, 1:1 acetonitrile/*tert*-butyl alcohol; TG6, 1:1 chloroform/ethanol.

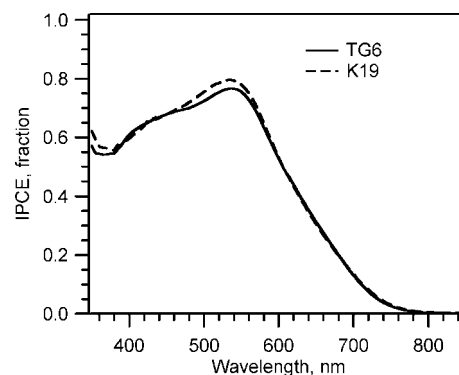


Figure 2. Spectral response (IPCE) of cells with K19 and TG6. TiO_2 film thickness $\approx 4 \mu\text{m}$. Electrolyte as in text.

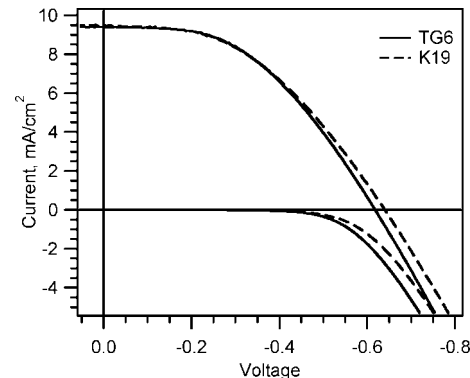


Figure 3. I - V results for cells with K19 and TG6. TiO_2 film thickness $\approx 4 \mu\text{m}$. Electrolyte as in text. Note that the low fill factors are due to the large active area (1 cm^2), low conductivity glass ($15 \Omega/\square$), and geometry of the cells.

($\sim 15\%$), the internal quantum efficiency is at least 90% for both dyes. This shows that at short circuit all the forward processes (injection, regeneration, and transport) are significantly faster than all the reverse processes (decay of the excited state, electron recombination to the dye, and electron recombination to the electrolyte).

Figure 3 gives typical photocurrent–voltage (I - V) results comparing the two dyes. The photocurrent is the same; however, the open-circuit photovoltage is $\sim 20 \text{ mV}$ larger for K19. The difference in voltage between the two dyes has been reproduced in additional comparisons using two different TiO_2 sources and two different electrolytes. Thus, this voltage difference seems to be an inherent effect of the dye structure. Losses in voltage are sometimes ascribed to dye aggregation on the TiO_2 surface.

(27) Bisquert, J. *J. Phys. Chem. B* **2004**, *108*, 2323.

(28) Salvador, P.; Hidalgo, M. G.; Zaban, A.; Bisquert, J. *J. Phys. Chem. B* **2005**, *109*, 15915.

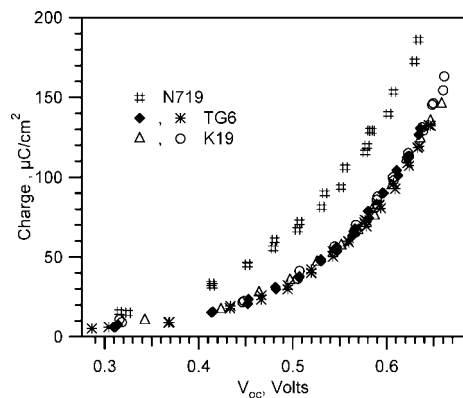


Figure 4. Charge in the cell as a function of V_{oc} .

Coadsorbates such as chenodeoxycholic acid (Cheno) can be added to the dye solution to reduce aggregation on the surface. We have made TG6 cells using (separately) Cheno, phenylpropionic acid, and octylphosphonic acid in the dye solutions. None of the additives caused an increase in voltage observed relative to the case of no additive. It seems likely that aggregation effects are not the source of the voltage difference between K19, TG6, and N719.

Figure 4 shows the excess charge present in the cells at V_{oc} , where the V_{oc} was varied by changing the bias light intensity. The charge follows an exponential increase with voltage, $Q = Q_0 e^{\beta V}$, with $\beta \approx 9.5$. The data show that the charge at V_{oc} is essentially identical for the TG6 and K19 cells. This result indicates that the conduction band edge is at the same potential (relative to iodine/iodide) for cells with both these dyes.²⁹ The charge vs V_{oc} curve for TG6 and K19 is shifted to ~ 60 mV higher voltages than for the reference dye, N719. This shift can be interpreted as a 60 mV upward shift in the conduction band. This shift is probably due to a change in ion access to the surface due to the bulkier substituents on K19 and TG6. The electron lifetime at V_{oc} , as a function of the V_{oc} , is shown in Figure 5a. As in Figure 4, the V_{oc} was controlled by the bias light intensity. At all voltages, the TG6 dye shows a recombination lifetime that is around one-half of that for K19. A similar N719 cell is also shown which has a lifetime about 3 times longer than that of K19 and 6 times longer than that of TG6. In order to more correctly compare electron lifetimes between cells, it is better to plot the lifetime vs the charge density (Figure 5b). In Figure 5b, there is only a slight shift in the relative positions of K19 and TG6, as expected since the charge is the same. However, we can see that the difference between both K19 and TG6 and N719 is larger than that implied by Figure 5a. In this particular cell composition (electrolyte and TiO_2 source), TG6 appears to have a lifetime about 15 times shorter than that of N719, which falls within the range (8–30) we have observed previously.¹²

The conclusion from Figures 4 and 5 is that the recombination lifetime at constant charge is shorter by a factor of 2.3 for TG6 relative to K19. This means that k'_o in the overall recombination rate equation $J_{rec} = k'_o n^{3.6}$ (see Introduction) has increased by a factor of 2.3 for TG6. We can check this data for consistency with the $I-V$ results, where TG6 shows 20 mV lower V_{oc} . Because the flux of injected electrons at V_{oc} is the same for both dyes (J_{sc} is the same, and see the text for Figure 7) it follows that J_{rec} does not change. In that case, n must decrease

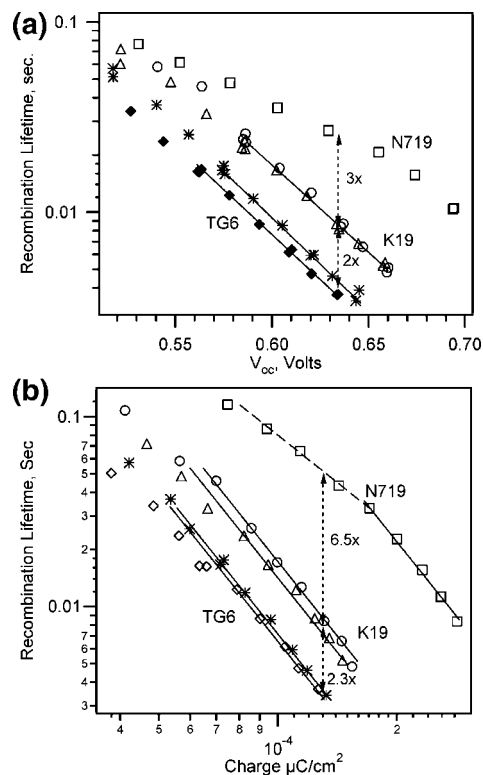


Figure 5. (a) Recombination lifetimes for DSSCs with various dyes vs V_{oc} . Lifetimes shown are the corrected steady-state lifetimes, τ_{ss} (see Experimental Section). (b) Recombination lifetimes for the same cells vs excess charge content of the cell.

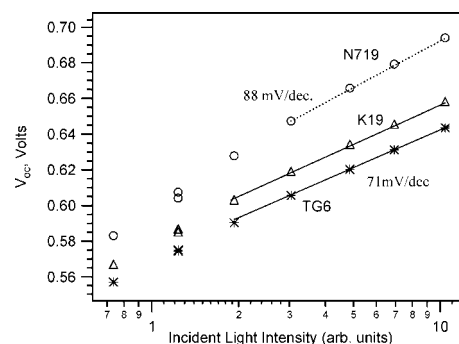


Figure 6. Open-circuit voltage as a function of light intensity. Illumination from white LEDs.

when k'_o increases. A 2.3-fold increase in k'_o will give a 1.26-fold decrease in n . Using the data in Figure 4, we can calculate what decrease in V_{oc} will be caused, using $V - V' = \ln(n/n')/9.5$. The result is -24 mV, in good agreement with the $I-V$ data.

Figure 6 shows the V_{oc} vs $\log(I_0)$, where I_0 is the incident light intensity on the cell. The slope of the line gives the “ideality” of the cell, where 60 mV/decade corresponds to an ideality equal to one. Here again, K19 and TG6 show very similar behavior. The ideality is related to how fast the recombination rate constant decreases as the light level and V_{oc} are decreased. Although the factors determining the ideality remain a mystery, it is likely related to the trap state characteristics of the surface, and/or the degree to which charges in solution can reach the surface and screen the electrons. For the purpose of comparing TG6 and K19, we note that the very similar ideality indicates that none of these parameters has

(29) O'Regan, B. C.; Scully, S.; Mayer, A. C.; Palomares, E.; Durrant, J. *J. Phys. Chem. B* **2005**, *109*, 4616.

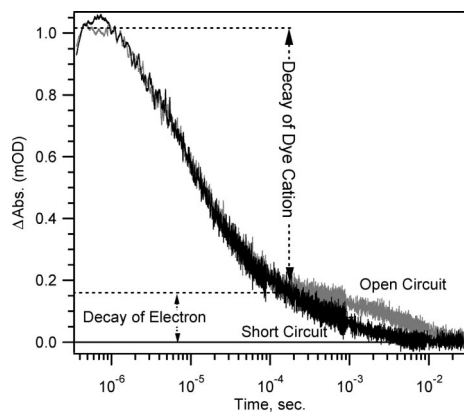


Figure 7. Transient absorbance decays for a K19 DSSC under white light bias. Pump, nitrogen dye laser at 630 nm. Probe, 800 nm.

changed. From this we can conclude further that the change in recombination rate constant is not related to changes in how the dye molecules pack on and interact with the surface. Conversely, TG6 and K19 both have a lower ideality factor than N719. The fact that the dye structure is one of the factors determining the ideality is a new and somewhat surprising observation. The trend between TG6 and N719 is reproducible, and the ideality of K19/TG6 cells is more reproducible than that of N719 cells. It is tempting to speculate that the iodine binding is directly affecting the ideality as well as the recombination rate. The phthalocyanines discussed in our previous paper show even lower voltages, presumably higher iodine binding, and also lower ideality factors. However, there are many other changes in dye structure occurring between N719, K19/TG6, and phthalocyanines, so caution is required.

In N719-based dye-sensitized cells the recombination flux at short circuit and at V_{oc} is mainly the reaction of the electron with the iodine in the electrolyte. It can be shown (see below) that the recombination of the electron with the oxidized dye is a minor contributor. We have found that this conclusion is still valid for TG6 and K19. Figure 7 shows the results of a transient absorption (TA) study on K19. The TA decays were measured with a probe of 820 nm, where the oxidized species of the dye, and the electron in the TiO_2 , both absorb. The cells were illuminated with ~ 1 sun white light intensity during the TA experiment. The two traces were taken with the cell at short circuit and open circuit. The early and fast part of the decay (to $\sim 100 \mu s$) is the disappearance of the dye cation, and the later part is the disappearance of the electron. At short circuit, because of the high IPCE of the cell, we know that at most only a small fraction of the electrons recombine with the oxidized dye, so the decay of the oxidized dye absorbance corresponds to the time scale of regeneration alone. At V_{oc} , the electron concentration in TiO_2 is about 10 times higher than at short circuit. However, the TA decay up to $100 \mu s$ is identical. If the increased electron concentration at V_{oc} had caused a significant increase in the fraction of electrons recombining with the oxidized dye, then the total decay rate should have increased, moving the TA decay to shorter times. As this did not happen, we can assume that for K19 cells the main reaction occurring at V_{oc} is still the recombination of electrons with the electrolyte. TG6 gave essentially identical results. The second part of the TA signal in Figure 7, due to the electrons, decays much faster at short circuit ($\tau_{tr} \approx 0.9 \mu s$) than at V_{oc} ($\tau_{tr} \approx 6$ ms). This is because the electrons can leave the TiO_2 as photocurrent at short circuit but can only decay by recombination with iodide at open circuit.

Consistent with this, the recombination lifetime at the 1 sun V_{oc} , measured electronically, is $\tau_{tr} = 5$ ms (Figure 5), and the photocurrent transient decay time is 1 ms (data not shown).

Discussion

The attraction of this class of dyes lies in the higher absorption coefficient relative to N719. However, this advantage comes with a cost in terms of V_{oc} relative to N719. Figure 5 shows that the extra ligands dramatically increase the recombination rate relative to N719. We have previously discussed the differences between N719 and TG6. The large changes in structure between N719 and TG6/K19 make it difficult to determine the exact cause of the increased recombination. The two-atom change between K19 and TG6 allows a much more definitive analysis. Figure 5 shows that the replacement of oxygen by sulfur alone causes a 2-fold increase in the recombination rate constant, k'_r . On the other hand, the other figures show that all other processes and conditions in K19 and TG6 are virtually identical. Figures 2 and 3 indicate that the injection efficiency and regeneration efficiencies are the same. With Figure 7 this indicates that the recombination with the dye does not contribute to the V_{oc} , and thus cannot contribute to a change in V_{oc} . Figure 4 shows that the band edge potential of the TiO_2 is the same for both dyes. The latter finding shows that the electric field between the TiO_2 and the electrolyte is the same in both cases; thus, the driving force for recombination is not changed. In sum, it is reasonable to conclude that the change in recombination rate constant is the sole contributor to the change in the V_{oc} , and that the single-atom change is the sole contributor to the change in rate constant.

We have previously hypothesized that increased iodine binding to the dye may be responsible for the large increases in recombination rate (relative to N719) in TG6, phthalocyanines, and even most organic dyes.^{5,12} If so, then we could expect that a difference in the tendency to bind iodine might be responsible for the smaller difference between K19 and TG6. Iodine is known to form charge-transfer complexes with many donors. The iodine binding constants for a large number of molecules have been published, including a large compilation table in ref 30. We suggest viewing the reported values as qualitative, as there can be a large variation between different authors. The reported iodine binding constant of ethylether is ~ 6 , whereas that for ethylthioether is ~ 200 (L/mol, in *n*-heptane, at 20 °C),^{31,32} a difference of 30-fold. Both these molecules are thought to bind iodine at the heteroatom lone pair. A contributor to the larger binding of the thioether is the lower electron affinity of sulfur (2.58) compared to oxygen (3.44). Lower electron affinity correlates with a greater ability as a donor.

When ether or thioether is connected to conjugated carbon systems, the lone pair can delocalize, decreasing the binding overall. This is demonstrated by the lower iodine binding of phenyl ethyl ether ($K \approx 0.35$) and phenyl ethyl thioether ($K \approx 9$).³³ Note, however, that the ratio between the sulfur and oxygen compound has not changed. If applicable to the dyes TG6 and K19, this ratio might be expected to give a larger change in the recombination rate than the factor 2 actually seen. We suspect, however, that as the lone pair is further delocalized into the

(30) Rao, C. N. R.; Chat, S. N.; Dwedi, P. C. *Appl. Spectrosc. Rev.* **1972**, 5, 1.

(31) Tamres, M.; Brandon, M. *J. Am. Chem. Soc.* **1960**, 82, 2134.

(32) Tsubomura, H.; Lang, R. P. *J. Am. Chem. Soc.* **1961**, 83, 2085.

(33) Wayland, B. B.; Drago, R. S. *J. Am. Chem. Soc.* **1964**, 86, 5240.

larger π system, the binding for K19 cannot fall much below ~ 0.35 , as the binding constant for benzene is on this same order. Steric hindrance must also play a role. The binding constant for bipyridine is reported to be ~ 90 .³⁴ The fact that N719 gives acceptable voltages implies that the binding to the bipyridine in the dye is far lower. Presumably a version of K19 without a heteroatom donor would still accelerate recombination somewhat relative to N719; however, it is also possible that this dye would not inject well due to the lower lying π orbitals on the ligand which is not attached to the TiO_2 . We note that we have found no literature on I_3^- binding to donors, and I_3^- acts as a donor itself in forming I_5^- . Thus, we have neglected the possibility that the dye might bind I_3^- , although we do not reject this as a possibility for future investigation.

Our data do not directly indicate how the binding of iodine to the dye increases the recombination rate. There are two possible mechanisms, both of which could operate together. Referring to the rate equation, $J_{\text{rec}} = k_{\text{or}} \alpha [\text{I}_{\text{os}}]^2$, the binding of iodine near the surface will increase $[\text{I}_{\text{os}}]$, and thus the rate. In iodine-iodide electrolyte, especially in nonaqueous electrolytes such as those used here, there is a strong complexation between I_2 and I^- , to form I_3^- . The binding constant in acetonitrile has been reported to be $\geq 10^6$.¹⁶ In these DSSC cells, iodide is in 10-fold excess, indicating that there is very little free iodine present in the cell. It has been found that the recombination reaction proceeds mainly via the reduction of I_2 , rather than I_3^- .¹⁹ In this case, recombination could well be limited by the concentration of I_2 within the reaction distance of the surface. Binding of iodine to the dye will create a larger concentration of the iodine near the surface, which can increase the recombination rate. It is, however, true that surface binding can only be a significant contribution to recombination if the exchange flux between iodine in tri-iodide and the iodine on the dye is larger than the recombination flux. Otherwise, the iodine on the dye will be depleted. Iodine/tri-iodide self-exchange is likely very fast; however, the binding time to the dye has still to be determined.³⁵ We note that it has been stated in the literature that the presence of species which bind iodine weakly (the example used was TBP) will lower the bulk iodine concentration in the electrolyte.³⁶ However, this is not correct. The high concentration of I_3^- acts as a buffer for the I_2 concentration. Species which bind I_2 much more weakly than does I^- will not perturb the bulk I_2 concentration.

Alternatively, it might be the case that recombination is limited by the activation barrier of the first step in the reduction of either iodine or tri-iodide. If binding to the dye can decrease this barrier, then recombination can proceed faster for a given iodine concentration. In this case there will be an increase in k_0 in the rate equation, as well as in $[\text{I}_{\text{os}}]$. One could speculate that iodine binding to the dye stabilizes the first reduction product of iodine, $\text{I}_2^{\bullet-}$. If $\text{I}_2^{\bullet-}$ is immobilized on a dye, thus preventing its rapid disproportionation in the bulk, it can accept another electron from the TiO_2 . Otherwise, the disproportionation of $\text{I}_2^{\bullet-}$ ($\leq 10 \mu\text{s}$ under operating conditions in these cells) will keep the concentration very low.³⁷

It is an important question to what extent N719 also binds iodine. As mentioned above, bipyridine binds iodine strongly

($K \approx 90 \text{ L/mol}$);³⁴ however, the literature indicates that in pyridine compounds the iodine binds directly to the nitrogen lone pair. Benzene and biphenyl bind iodine only weakly (0.25 and 0.36). It would seem likely that, between the binding of the nitrogens to the ruthenium and steric hindrance between the ligands, iodine binding to N719 is likely to be weak. With respect to recombination studies of N719, we have no reference dye guaranteed not to bind iodine, so the effect of N719 on recombination can only be examined indirectly. The recombination rate constant of bare TiO_2 films, illuminated with UV light, probably cannot serve as an adequate reference, as UV light causes other effects at the TiO_2 surface.^{38,39} A suggested method to compare recombination is to compare the dark $I-V$ with and without dye. In this test, N719 sometimes appears to “block” the surface, decreasing the dark current, and sometimes shows equivalent dark current to bare TiO_2 (data not shown). However, it is virtually certain that N719 will shift the conduction band relative to the no-dye case, leaving any dark current comparisons in doubt. We have developed a charge extraction experiment to measure the charge density of the TiO_2 film in the dark. Data comparing N719-coated and bare TiO_2 will be presented in the future. Beyond this, however, even bare TiO_2 contains oxygen “donor” sites and is likely to adsorb iodine as well. All that can be said at this time is that combined effects of N719 on the band edge and on iodine adsorption approximately cancel to give little difference from bare TiO_2 .

An even more important question concerns the modification of candidate dye structures to reduce iodine binding. Several approaches may be useful. As mentioned above, the oxygen or sulfur atoms in K19 and TG6 are present in order to donate electron density to the extended π system on the ligand. A rather strong donation appears to be necessary, so the heteroatoms cannot simply be removed. However, it might be possible to add a larger number of weaker donors, instead of one strong donor. The increase in overall π system density will likely still increase binding (e.g., hexamethyl benzene (1.5) relative to benzene (0.25) but perhaps to a lesser degree than a heteroatom with a lone pair). A second approach could be to build in steric hindrance at key points. The following series of pyridine derivatives shows the effects of steric hindrance around a pyridine nitrogen: pyridine ($K = 60-160 \text{ L/mol}$), 2,5-dimethylpyridine ($K \approx 129$) versus 2,6-dimethylpyridine ($K \approx 30$) versus 2-methyl-6-styrylpyridine ($K \approx 6$).³⁰ Note the decrease in the last compound comes about despite the increase in the π system size. Lastly, binding of iodine to multiple heteroatoms incorporated into conjugated ring structures follows a complex set of rules that may be exploited once iodine binding is recognized as a problem. In sum, it should be possible to design a lack of iodine binding into candidate dyes. If dyes can be made which bind iodine less strongly than TiO_2 and/or N719, it may yet be possible to increase both the red response and the voltage.

Conclusions

We have shown that a two-atom change in a dye structure can have significant effects on the recombination rate and through that on the cell V_{oc} . Combined with literature values for iodine complexation, the results suggest very strongly that iodine, or possibly tri-iodide, binding to the dye is the cause of the difference. What we have not been able to show is the iodine

(34) Rao, N. S.; Rao, G. B.; Ziessow, D. *Spectrochim. Acta* **1990**, *46A*, 1107.

(35) Ruasse, M. F.; Aubard, J.; Galland, B.; Adenier, A. *J. Phys. Chem.* **1986**, *90*, 4382.

(36) Boschloo, G.; Hagman, L.; Hagfeldt, A. *J. Phys. Chem. B* **2006**, *110*, 13144.

(37) O'Regan, B. Unpublished data.

(38) O'Regan, B.; Schwartz, D. T. *Chem. Mater.* **1998**, *10*, 1501.

(39) Ferrere, S.; Gregg, B. A. *J. Phys. Chem. B* **2001**, *105*, 7602.

binding constant for the two dyes. We have started a project to measure iodine binding to dyes and other components in the cell, but the measurement is not simple. For example, the IR, Raman, and UV–vis spectra of iodine complexes are known to evolve with time, often for days.⁴⁰ Indeed, we find this behavior for methoxypropionitrile, the solvent for the cell electrolyte. Since similar evolution is often seen in the cell I – V results, iodine complexation may have effects well beyond the ones measured here. The significance of this, if true, should be very wide ranging. Elucidation of the iodine complexation with

the dye, electrolyte, and TiO_2 is a critical goal for further understanding and improvement of DSSCs.

Acknowledgment. This work was supported by the UK EPSRC (Grant EP/E035175/1), the EU Seventh Framework Program Grant Number 212792, the University Research Board (URB) at the American University of Beirut (AUB), and the Lebanese National Council for Scientific Research (LNCSR).

Supporting Information Available: Full author list of ref 2. This material is available free of charge via the Internet at <http://pubs.acs.org>.

JA806869X

(40) Tassaing, T.; Besnard, M. *J. Phys. Chem. A* **1997**, *101*, 2803.